CrossMark

JM PAPERS

Instability of a dusty Kolmogorov flow

Alessandro Sozza[1,2,3,4,†], Massimo Cencini[2,3], Stefano Musacchio[1] and Guido Boffetta[1]

[1]Department of Physics and INFN, University of Torino, via P. Giuria, 10125 Torino, Italy

[2]Istituto dei Sistemi Complessi, ISC-CNR, via dei Taurini 19, 00185 Roma, Italy

[3]INFN sezione Roma 2 "Tor Vergata", Via della Ricerca Scientifica 1, 00133 Roma, Italy

[4]Laboratoire de Physique, UMR 5672, École Normale Supérieure de Lyon 46 Allée d'Italie, 69007 Lyon, France

Suspended particles can significantly alter the fluid properties and, in particular, can modify the transition from laminar to turbulent flow. We investigate the effect of heavy particle suspensions on the linear stability of the Kolmogorov flow by means of a multiple-scale expansion of the Eulerian model originally proposed by Saffman (*J. Fluid Mech.*, vol. 13, issue 1, 1962, pp. 120–128). We find that, while at small Stokes numbers particles always destabilize the flow (as already predicted by Saffman in the limit of very thin particles), at sufficiently large Stokes numbers the effect is non-monotonic in the particle mass fraction and particles can both stabilize and destabilize the flow. Numerical analysis is used to validate the analytical predictions. We find that in a region of the parameter space the multiple-scale expansion overestimates the stability of the flow and that this is a consequence of the breakdown of the scale separation assumptions.

Key words: suspensions, particle/fluid flow

1. Introduction

Particles transported in flow are ubiquitous in many natural environments, from protoplanetary disks (Armitage 2011) to aerosol in the atmosphere (Shaw 2003), from volcanic eruptions (Bercovici & Michaut 2010) to sediment transport (Burns & Meiburg 2015).

Dispersed particles are not only transported by the flow, but they exert forces on the fluid that, depending on the mass loading, can modify the flow itself. As discovered long ago (Sproull 1961), at high Reynolds numbers heavy particles can alter turbulence by attenuating or enhancing it depending on their size and mass fraction and on the

scale considered (Balachandar & Eaton 2010; Bec, Laenen & Musacchio 2017; Gualtieri, Battista & Casciola 2017). In channel flow, they can change the turbulent drag (Ardekani *et al.* 2017; Li *et al.* 2019). At low Reynolds numbers, the presence of particles affects the stability of laminar flow and the transition to turbulence. Indeed, as first realized by Saffman (1962), tiny particles, characterized by small Stokes number, typically anticipate the onset of the instability while coarser ones retard it. This intuition was later confirmed by other studies in the context of pipe (Michael 1964; Rudyak, Isakov & Bord 1997) and channel (Klinkenberg, De Lange & Brandt 2011) flows. However, in wall bounded flows the analysis is complicated by the interaction of particles with the boundaries and by the fact that the transition is subcritical and thus finite amplitude perturbations are required to destabilize the flow.

In this work we study the effects of a particle suspension on the stability of a periodic Kolmogorov flow. This sinusoidal flow was proposed by Kolmogorov as a simple model to understand the transition to turbulence and, after seven decades of study, it is still a attracting a broad scientific interest (for a recent review see, e.g. Fylladitakis 2018). From a theoretical point of view, it has the advantage, with respect to other parallel shear flows, of being analytically tractable for the study of its linear stability and weakly nonlinear dynamics (Sivashinsky 1985). In numerical simulations, it is widely used as a prototype of shear flow with periodic boundary conditions which can be easily implemented in pseudo-spectral codes. Moreover, the Kolmogorov flow can be considered as a simplified channel flow without boundaries, since it displays a mean velocity profile which remains monochromatic even in the turbulent regime (Musacchio & Boffetta 2014). For these reasons, analytical and numerical studies have extended the Kolmogorov flow to rotating (Legras, Villone & Frisch 1999), stratified (Balmforth & Young 2002) and viscoelastic flows (Boffetta, Celani & Mazzino 2005). We recall that, beside the numerical and analytical studies, the Kolmogorov flow is also realizable in experiments (Suri *et al.* 2014). Recently, the Kolmogorov flow has been also used to study numerically the clustering of inertial particles (De Lillo *et al.* 2016; Pandey, Perlekar & Mitra 2019) as well as the effect of a heavy particle suspension on turbulent drag (Sozza *et al.* 2020). The latter numerical study was performed by using an Eulerian approach originally developed by Saffman (1962), valid in the limit of small volume fraction for mono-disperse heavy particle suspensions.

In the present work we consider the laminar stationary solution of the Saffman model forced by a Kolmogorov flow. We show that it is possible to study the stability problem perturbatively, by exploiting a multiple-scale expansion (Bensoussan, Lions & Papanicolaou 2011). The analytical result, which extends the Newtonian one (Sivashinsky & Yakhot 1985), predicts a rich phenomenology with both enhanced and reduced stability as a function of the control parameters, namely the particle Stokes number and mass fraction. In particular, we confirm the known phenomenology that tiny (coarse) particles tend to destabilize (stabilize) the flow with respect to the Newtonian case. Moreover, we show that for coarse enough particles the effect is non-monotonic in the mass fraction: at small mass fractions the flow is stabilized while it is destabilized at large enough mass fractions. A similar phenomenology was observed for neutrally buoyant particles in pipe flows (Matas, Morris & Guazzelli 2003; Agrawal, Choueiri & Hof 2019). We compare the analytically predicted critical Reynolds number with the results of an extended numerical investigation and we explain the observed discrepancies for some values of the parameters with the breakdown of the scale separation assumption.

The remainder of this paper is organized as follows. In § 2 we introduce the Saffman model. In § 3 we perform the linearization around the Kolmogorov base flow. Section 4 is

devoted to the multiple-scale approach for the linear stability problem. In § 5 we discuss the dependence of the critical Reynolds number on the control parameters and compare the analytical predictions with the numerical results. Finally, § 6 is devoted to the conclusions.

2. Saffman model for a dusty Kolmogorov flow

We consider an Eulerian model for a dilute suspension of heavy particles with two-way coupling introduced by Saffman (1962) long ago. The model considers a dilute mono-disperse suspension of small, heavy, spherical particles with density ρ_p and radius a transported by a Newtonian fluid with density ρ_f and viscosity μ. Particle size is assumed to be much smaller than any scale in the flow such that the particle Reynolds number is negligible. The particle volume fraction $\phi_v = N_p v_p / V$, defined in terms of the volume of each particle $v_p = 4\pi a^3/3$ and the number of particles N_p contained in the total volume V, is assumed to be negligible while the mass fraction $\phi = \phi_v \rho_p / \rho_f$ can be of order one since it is assumed $\rho_p \gg \rho_f$ (as in a dilute suspensions of water droplets in air).

Within the model, the fluid density field remains constant because of the assumption of vanishing ϕ_v and it is transported by the incompressible velocity field of the fluid phase $\boldsymbol{u}(\boldsymbol{x}, t)$. The solid phase is described by a number density field $\theta(\boldsymbol{x}, t) = n(\boldsymbol{x}, t)/(N_p/V)$, where $n(\boldsymbol{x}, t)$ is the local number of particles per unit volume. The normalization gives $\langle \theta \rangle = 1$, where the brackets $\langle [\cdot] \rangle$ denote the average over the volume V. The number density field θ is transported by a compressible particle velocity field $\boldsymbol{v}(\boldsymbol{x}, t)$.

For small volume fractions ($\phi_v < 10^{-3}$) the dynamics of the particle-laden flow can be described by a two-way coupling, which takes into account the interactions between individual particles and the surrounding flow, but neglects the interactions between particles (collisions and friction) and the particle–fluid–particle interactions (fluid streamlines compressed between particles) (Elghobashi 1994). In the two-way coupling regime, the exchange of momentum between the two phases can no longer be neglected (Balachandar & Eaton 2010). For small heavy particles, such an exchange is mainly mediated by the viscous drag force which is proportional to the difference between particle and fluid velocities.

The accurate modelling of the coupling between the particles and the flow is a challenging task. In Lagrangian–Eulerian approaches based on the point-particle method, it requires taking into account the local perturbation to the fluid due to the presence of the particle (Horwitz & Mani 2016). The Eulerian model proposed by Saffman is based on a simplified assumption, namely that the coupling is obtained by imposing the local conservation of the total momentum of the fluid and particle phases. This leads to the following equations (Saffman 1962):

$$\partial_t \boldsymbol{u} + \boldsymbol{u} \cdot \nabla \boldsymbol{u} = -\nabla p + \nu \nabla^2 \boldsymbol{u} + \boldsymbol{f} + \frac{\phi}{\tau}\theta(\boldsymbol{v} - \boldsymbol{u}), \quad (2.1)$$

$$\partial_t \boldsymbol{v} + \boldsymbol{v} \cdot \nabla \boldsymbol{v} = -\frac{1}{\tau}(\boldsymbol{v} - \boldsymbol{u}), \quad (2.2)$$

$$\partial_t \theta + \nabla \cdot (\boldsymbol{v}\theta) = 0, \quad (2.3)$$

where $\tau = (2/9)a^2 \rho_p / (\rho_f \nu)$ is the relaxation time of the particles, $\nu = \mu / \rho_f$ is the kinematic viscosity, p is the pressure and $\boldsymbol{f}$ is an external forcing.

In the limit of very tiny particles, i.e. small τ, the Saffman model reduces to the Navier–Stokes equation for an incompressible flow with an increased density, and thus a smaller viscosity (Saffman 1962). Indeed, when $\tau \to 0$ from (2.2) one has $\boldsymbol{v} = \boldsymbol{u}$.

For small τ one can expand $\boldsymbol{v} = \boldsymbol{u} + \tau\tilde{\boldsymbol{v}} + O(\tau^2)$ and (2.2) gives, at leading order, $\tilde{\boldsymbol{v}} = -(\partial_t\boldsymbol{u} + \boldsymbol{u}\cdot\nabla\boldsymbol{u}) + O(\tau)$. Substituting now $\boldsymbol{v} = \boldsymbol{u} - \tau(\partial_t\boldsymbol{u} + \boldsymbol{u}\cdot\nabla\boldsymbol{u})$ in (2.3) one obtains that the particle density field remains constant at leading order. Finally, using $\theta = 1 + O(\tau)$ and $(\boldsymbol{v} - \boldsymbol{u})/\tau = -(\partial_t\boldsymbol{u} + \boldsymbol{u}\cdot\nabla\boldsymbol{u}) + O(\tau)$ in (2.1) gives

$$\partial_t\boldsymbol{u} + \boldsymbol{u}\cdot\nabla\boldsymbol{u} = -\nabla p + \frac{\nu}{1+\phi}\nabla^2\boldsymbol{u} + \frac{\boldsymbol{f}}{1+\phi}, \qquad (2.4)$$

i.e. the Navier–Stokes equation for an incompressible velocity field with forcing and viscosity rescaled by the factor $(1+\phi)$.

Remarkably, we show that the same result is also recovered in the limit of large ϕ. Indeed, from (2.1) one can write

$$\boldsymbol{u} = \boldsymbol{v} + \frac{\tau}{\phi}\frac{1}{\theta}\left(-\partial_t\boldsymbol{u} + \boldsymbol{u}\cdot\nabla u - \nabla p + \nu\nabla^2\boldsymbol{u} + \boldsymbol{f}\right), \qquad (2.5)$$

showing that the difference between $\boldsymbol{u}$ and $\boldsymbol{v}$ is of order $1/\phi \ll 1$. Substituting $\boldsymbol{v} = \boldsymbol{u} + O(1/\phi)$ in (2.3) implies $\theta = 1 + O(1/\phi)$ which, together with (2.5) in (2.2), yields (2.4) multiplied by $(1+\phi)$, i.e. again a Navier–Stokes equation with rescaled forcing and viscosity. We remark that the limit of large ϕ is physically questionable since it could violate the assumption of negligible volume fraction. Nonetheless, it is mathematically well defined and we will use it the following to discuss our results.

We consider the case of a monochromatic periodic forcing $\boldsymbol{f} = F\cos(Ky)\hat{\boldsymbol{x}}$ which produces the Kolmogorov laminar fixed point $\boldsymbol{u}(\boldsymbol{x}) = \boldsymbol{v}(\boldsymbol{x}) = U(y) \equiv U\cos(Ky)$ with $U = F/(\nu K^2)$ and $\theta(\boldsymbol{x}) = 1$. We remark that, in general, the Kolmogorov flow is a stationary solution also for $\theta(\boldsymbol{x}) = g(y)$ with g an arbitrary function. Nonetheless, the solution with uniform density θ is physically the more relevant as it survives in the presence of an arbitrarily small diffusivity.

The non-dimensional parameters of the model are the Reynolds number $Re = U/(\nu K)$, defined in terms of the amplitude of the laminar flow U and on the only characteristic length of the flow K^{-1}, the Stokes number $St = \tau\nu K^2$, defined as the ratio between the particle relaxation time τ and the viscous time $\tau_\nu = 1/(\nu K^2)$ and the mass fraction ϕ. In the following, we will study the linear stability of the laminar fixed point as a function of Re, St and ϕ.

We conclude this section with a comment about the limitations of the Saffman model. Beside the assumption of small volume fraction, in the case of turbulent flows at high Reynolds numbers the validity of the model (2.1)–(2.3) is in general limited to small Stokes numbers $St < 1$. This is due to the phenomenon of caustics (Wilkinson & Mehlig 2005) which would imply a multi-valued particle velocity field breaking the validity of the continuum description. Nonetheless, for the specific case of the linear stability of a laminar parallel flow considered here, in the laminar fixed point the particle velocity field is equal to the fluid velocity field, and therefore the model is well defined for arbitrary value of St.

3. Linear stability analysis

We study the linear stability of an infinitesimal perturbation of the basic Kolmogorov flow. To this aim we expand (2.1)–(2.3) around the laminar fixed point $\boldsymbol{u}(\boldsymbol{x},t) = U(y) + \boldsymbol{u}'(\boldsymbol{x},t)$, $\boldsymbol{v}(\boldsymbol{x},t) = U(y) + \boldsymbol{v}'(\boldsymbol{x},t)$, $\theta(\boldsymbol{x},t) = 1 + \theta'(\boldsymbol{x},t)$, and obtain the linearized

equations for the perturbations

$$\partial_t \boldsymbol{u}' + \boldsymbol{U} \cdot \nabla \boldsymbol{u}' + \boldsymbol{u}' \cdot \nabla \boldsymbol{U} = -\nabla p' + \nu \nabla^2 \boldsymbol{u}' + \frac{\phi}{\tau}(\boldsymbol{v}' - \boldsymbol{u}'), \tag{3.1}$$

$$\partial_t \boldsymbol{v}' + \boldsymbol{U} \cdot \nabla \boldsymbol{v}' + \boldsymbol{v}' \cdot \nabla \boldsymbol{U} = -\frac{1}{\tau}(\boldsymbol{v}' - \boldsymbol{u}'), \tag{3.2}$$

$$\partial_t \theta' + \boldsymbol{U} \cdot \nabla \theta' + \nabla \cdot \boldsymbol{v}' = 0. \tag{3.3}$$

We observe that, at this order, the density field becomes a passive scalar since it does not enter (3.1)–(3.2). Therefore, the evolution of θ' can be neglected.

A remarkable simplification of the linear stability analysis can be achieved by invoking the Squire theorem for parallel flows (Squire 1933), which states that it suffices to consider two-dimensional perturbations, since three-dimensional perturbations are more stable. From the original formulation, the theorem has been extended to various systems, including magnetohydrodynamic equations (Hughes & Tobias 2001), stratified flows (Balmforth & Young 2002) and viscoelastic flows (Bistagnino *et al.* 2007). In Appendix A, we report the derivation of the Squire theorem for the dusty fluid model (3.1)–(3.2).

In the following we will therefore consider the two-dimensional version of the linearized equation. It is convenient to rewrite the fluid velocity fluctuation in terms of a streamfunction $\boldsymbol{u}' = (\partial_y \Psi, -\partial_x \Psi)$ and the compressible particle velocity in terms of a particle streamfunction Ψ_p and potential Φ_p as $\boldsymbol{v}' = (\partial_y \Psi_p + \partial_x \Phi_p, -\partial_x \Psi_p + \partial_y \Phi_p)$. In terms of these fields the linear equations (3.1)–(3.2) read

$$\partial_t \nabla^2 \Psi + U \cos(Ky)(K^2 + \nabla^2)\partial_x \Psi - \nu \nabla^4 \Psi + \frac{\phi}{\tau}\nabla^2(\Psi - \Psi_p) = 0, \tag{3.4}$$

$$\partial_t \nabla^2 \Psi_p + U \cos(Ky)\left[(K^2 + \nabla^2)\partial_x \Psi_p - K^2 \partial_y \Phi_p\right] - Uk \sin(Ky)\nabla^2 \Phi_p + \frac{\nabla^2(\Psi_p - \Psi)}{\tau} = 0, \tag{3.5}$$

$$\partial_t \nabla^2 \Phi_p + U \cos(Ky)\partial_x \nabla^2 \Phi_p - 2UK \sin(Ky)\left(\partial_x \partial_y \Phi_p - \partial_x^2 \Psi_p\right) + \frac{1}{\tau}\nabla^2 \Phi_p = 0. \tag{3.6}$$

For a Newtonian fluid ($\phi = 0$), the laminar solution is known to be linearly stable to perturbations at wavenumbers larger than K, and to become unstable to large-scale transverse perturbations (i.e. in the direction x transverse to the direction of modulation z) above the critical value $Re_c = \sqrt{2}$ (Meshalkin & Sinai 1961; Sivashinsky & Yakhot 1985). As discussed in §2, in the limit of small inertia ($\tau \ll 1$) or large mass fraction ($\phi \gg 1$) the Saffman model recovers the Navier–Stokes equation with a rescaled viscosity $\nu/(1 + \phi)$. Therefore, in these limits we expect the critical Reynolds number to become $Re_c = \sqrt{2}/(1 + \phi)$, i.e. the presence of tiny particles, or a large mass fraction of particles, makes the flow more unstable.

4. Multiple-scale analysis

The general dependence of the critical Reynolds number on the parameters τ and ϕ can be obtained by a standard multiple-scale analysis (Bensoussan *et al.* 2011) of the linearized equations (3.4)–(3.6). The main idea of the multiple-scale method is to search for a perturbation which varies on spatial scales much larger than those of the base flow. For this purpose, beside the small-scale variables x, y and t, the multiple-scale method introduces the large-scale spatial variables $X = \varepsilon x$, $Y = \varepsilon y$ and a corresponding slow time

$T = \varepsilon^2 t$, where the small parameter ε is the ratio between the characteristic scales of the basic flow and the perturbation. The relative powers of ε in the space and time variables reflect the diffusive dynamics expected at large scales. The two sets of variables are then assumed to be independent, so that by averaging over the small scales it is possible to obtain an effective diffusion-like equation for the large scales, which defines an eddy viscosity. A change of sign of the eddy viscosity corresponds to a change of the stability of the perturbation. In particular, the system becomes unstable when the eddy viscosity becomes negative (Sivashinsky & Yakhot 1985; Dubrulle & Frisch 1991).

The choice of the multiple-scale method to study the stability of the dusty Kolmogorov flow is motivated by the fact that, in the Newtonian case (at $\phi = 0$), the most unstable perturbation is indeed at large scale, and the multiple-scale prediction for the critical Reynolds number is correct. For simplicity of the calculation, and in analogy with the Newtonian case, we also assume that the most unstable perturbation is transverse, i.e. depends on the large-scale variable X only and not on Y. The validity of these assumptions for the dusty gas at $\phi > 0$ will be checked by extensive numerical simulations of the linear systems in § 5. In particular, we anticipate that, while the transverse nature of the most unstable perturbation was always confirmed, in a certain parameter region the scale separation appears to be violated, when this happens the multiple-scale approach does not provide the correct prediction.

Before proceeding, it is convenient to rewrite (3.4) in terms of a co-streamfunction defined as $\chi = \Psi + \phi \Psi_p$. Such a choice allows us to remove the apparent singularity of the Stokes drag in the limit $\tau \to 0$ in (3.4). Indeed, by combining (3.4) and (3.5) we obtain

$$\partial_t \nabla^2 \chi + U \cos(Ky)(K^2 + \nabla^2)\partial_x \chi - \phi U K \left(K \cos(Ky)\partial_y \Phi_p + \sin(Ky)\nabla^2 \Phi_p \right)$$
$$- \nu \nabla^4 (\chi - \phi \Psi_p) = 0, \tag{4.1}$$

which removes the explicit dependence of (3.4) on τ. The linear systems for the perturbative analysis is hence formed by the set of equations (4.1), (3.5) and (3.6).

Following the multiple-scale method, we assume a perturbative expansion of the fields

$$\left.\begin{aligned}
\chi(X, y, T) &= \chi_0(X, y, T) + \varepsilon \chi_1(X, y, T) + \varepsilon^2 \chi_2(X, y, T), \\
\Psi_p(X, y, T) &= \Psi_{p,0}(X, y, T) + \varepsilon \Psi_{p,1}(X, y, T) + \varepsilon^2 \Psi_{p,2}(X, y, T), \\
\Phi_p(X, y, T) &= \Phi_{p,0}(X, y, T) + \varepsilon \Phi_{p,1}(X, y, T) + \varepsilon^2 \Phi_{p,2}(X, y, T).
\end{aligned}\right\} \tag{4.2}$$

The derivative operators are transformed as $\partial_x \to \varepsilon \partial_X$, $\partial_t \to \varepsilon^2 \partial_T$. Notice that the base flow does not depend on x and t and therefore the same holds for the perturbation. By inserting the expansions (4.2) and the fast/slow variable decomposition into (4.1), (3.5) and (3.6) we obtain, at order ε^0, that the zero-order fields do not depend on the fast variable, i.e. $\chi_0(X, y, T) = a_0(X, T)$, $\Psi_{p,0}(X, y, T) = b_0(X, T)$ and $\Phi_{p,0}(X, y, T) = c_0(X, T)$. At the order ε^2, the absence of secular terms requires $c_0 = 0$.

The solvability condition is obtained by integrating (3.5)–(4.1) over one period of the fast variable y. The first non-trivial condition is obtained at order ε^3 and gives a relation among the large-scale fields

$$a_0(X, T) = (1 + \phi)b_0(X, T). \tag{4.3}$$

At order ε^4, we finally get the diffusion equation for the slow field a_0

$$\frac{2}{Re}(1 + \phi)\partial_T \partial_X^2 a_0(X, T) + \nu Re \left(1 - \frac{2}{Re^2} + 2\phi + \phi^2 - \phi St \right) \partial_X^4 a_0(X, T) = 0, \tag{4.4}$$

which defines the eddy viscosity

$$\nu_e = \nu \frac{Re^2}{2(1 + \phi)} \left(\frac{2}{Re^2} - (1 + \phi)^2 + \phi St \right). \tag{4.5}$$

The critical Reynolds number is finally obtained by the condition $\nu_e = 0$ at which the eddy viscosity becomes negative, indicating that the basic flow is linearly unstable (Sivashinsky & Yakhot 1985; Dubrulle & Frisch 1991)

$$Re_c = \sqrt{\frac{2}{(1 + \phi)^2 - \phi St}}. \tag{4.6}$$

For $\phi = 0$ the critical Reynolds number predicted by (4.6) recovers correctly the Newtonian value $Re_c = \sqrt{2}$. Interestingly, the same value is recovered also on the neutral curve $St = 2 + \phi$. For $St \to 0$ we obtain the Saffman limit $R_c = \sqrt{2}/(1 + \phi)$. For $St < 2$, (4.6) predicts a monotonic decrease of Re_c as a function of ϕ ($Re_c(\phi) \le Re_c(0)$), indicating that tiny particles always destabilize the flow. On the contrary, for $St > 2$, the critical Re depends on ϕ in a non-monotonic way: for $\phi < \phi_{max} = (St - 2)/2$, Re_c increases monotonically above the Newtonian value $\sqrt{2}$, it reaches a maximum at ϕ_{max} after which it monotonically decreases and for $\phi > St - 2$ it goes below $\sqrt{2}$. Therefore, increasing the mass fraction particles first stabilize the flow up to a maximum then the stabilizing effect decreases and, finally, for large enough mass fraction particles make the flow more unstable than the in the Newtonian case. We remark that, according to (4.6), the dusty Kolmogorov flow should always be stable (i.e. $Re_c \to \infty$) for $St \ge (1 + \phi)^2/\phi \ge 4$. We will see that this is actually an overestimation of the stability due to the fact that the main assumption of the multiple-scale analysis (instability to large-scale perturbations) does not hold in a certain region of the parameter space (ϕ, St).

5. Numerical analysis

To check the validity of the analytical result (4.6) obtained with the multiple-scale analysis, we performed an extensive numerical study of the linearized equations in two dimensions (3.4)–(3.6) by means of a pseudo-spectral method in a square domain of size $L = 2\pi$ with periodic boundary conditions. For each set of values of the parameters ϕ and St in the range $0 \le \phi \le 6$ and $0 \le St \le 6$ we have studied the stability of the system on varying the Re number. The latter has been varied by changing the amplitude of the forcing F while keeping fixed the viscosity $\nu = 10^{-3}$ and the scale of the base flow $1/K$. Simulations were done at two different resolutions, with 128^2 and 256^2 grid points and forcing wavenumber $K = 32$ and $K = 64$, respectively, to check finite size effects. A random initial perturbation has been imposed on each Fourier mode (k_x, k_y) in the range $0 \le |\mathbf{k}| \le K$. The stability of each mode and its growth rate is determined by the temporal evolution of its amplitude after a short transient. The critical Reynolds number was determined by means of the bisection method based on the total kinetic energy of the fluid.

In figure 1(*a*) we plot the critical Reynolds number as a function of the Stokes number for different mass fraction values ϕ. At small St, Re_c is smaller than that of the single-phase fluid ($Re_c = \sqrt{2}$ for $\phi = 0$) and the numerical results are in agreement with the theoretical prediction (4.6). In particular, in the limit $St \ll 1$, the critical Reynolds number recovers the Saffman limit $Re_c = \sqrt{2}/(1 + \phi)$ (not shown). The critical Reynolds number increases monotonically with St at fixed ϕ, eventually becoming larger than $\sqrt{2}$, meaning that large
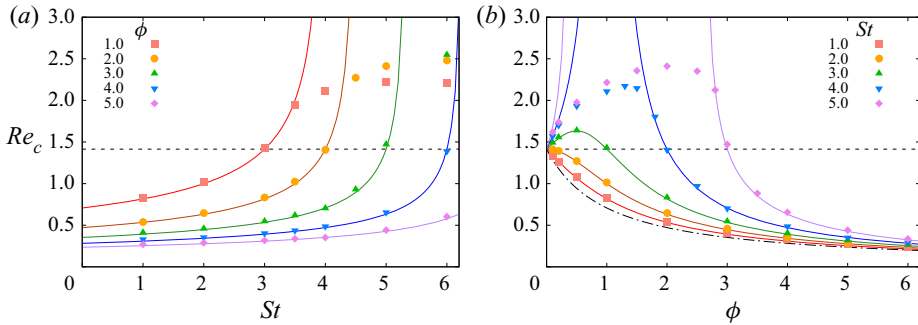
Figure 1. Critical Reynolds number (*a*) as a function of the Stokes number *St* for different values of ϕ and (*b*) as a function of the mass fraction ϕ for different values of *St*. The values of the parameters ϕ and *St* are reported in the legend. Solid curves denote the multiscale prediction (4.6); symbols the numerical results; dashed lines display the Newtonian value $\sqrt{2}$; dash-dotted line in panel (*b*) shows the Saffman limit $\sqrt{2}/(1+\phi)$.

particle inertia has a stabilizing effect on the flow. At a qualitative level, the physical mechanisms of the stabilizing/destabilizing effect of the particles have been already discussed by Saffman (1962). Particles with small *St* follow the flow almost like tracers, so that their effect is simply to increase the density of the suspension. Therefore, the dusty gas behaves as a Newtonian flow with a reduced kinematic viscosity (see (2.4)) which makes the flow more unstable. Conversely, particles with large inertia do not follow the perturbation of the flow, but they 'carry on with the velocity of the base flow' (Saffman 1962). The disturbance has therefore to flow around the particles, dissipating its energy because of the viscous drag. Our numerical results show that the stabilizing effect at large *St* is weaker than the prediction (4.6). In particular, the multiple-scale method predicts unconditioned stability (i.e. $Re_c = \infty$) for $St \geq (1 + \phi)^2/\phi$, while in the numerical simulations Re_c remains finite.

The behaviour of Re_c as a function of the mass fraction ϕ for fixed values of *St*, shown in figure 1(*b*), gives further insights into the stability of the system. In agreement with (4.6), we find that Re_c is monotonically decreasing for $St \leq 2$ (i.e. tiny particles always destabilize the flow). Conversely, at $St > 2$ the particles at low concentration stabilize the flow while at sufficiently large concentrations $\phi \geq St - 2$ they have a destabilizing effect. It is interesting to note that a similar non-monotonic behaviour as a function of the mass loading has been observed also for the skin-friction coefficient in Lagrangian–Eulerian simulations of inertial particles in a vertical channel flow (Capecelatro, Desjardins & Fox 2018). The physical mechanism of the destabilizing effect at large ϕ is similar to that of the case of small *St*. The strong drag exerted by the large mass fraction forces the fluid to follow closely the particle velocity (see (2.5)). As a consequence, the dusty gas behaves almost as a single-phase fluid with a larger density and therefore a smaller kinematic viscosity, which reduces its stability. From figure 1(*b*) it is evident that the agreement between the multiple-scale result and numerical simulations is very good for any ϕ up to $St = 3$. For $St \geq 4$, the multiple-scale result (4.6) overestimates the Re_c for an intermediate interval of values of ϕ around $\phi_{max} = (St - 2)/2$. Nonetheless, also in these cases ($St = 4$ and $St = 5$) the multiple-scale prediction works well for small and large values of ϕ.

In order to understand why the multiple-scale analysis fails in predicting the correct Re_c at large *St*, we computed numerically the growth rate σ as a function of the wavenumber k_x of the perturbation (i.e. the dispersion relation) for different values of the parameters ϕ and *St*. In figure 2(*a*) we show the dispersion relation computed at the critical point $Re = Re_c$ for $St = 4$ and three values of the mass fraction. For small and large mass fractions
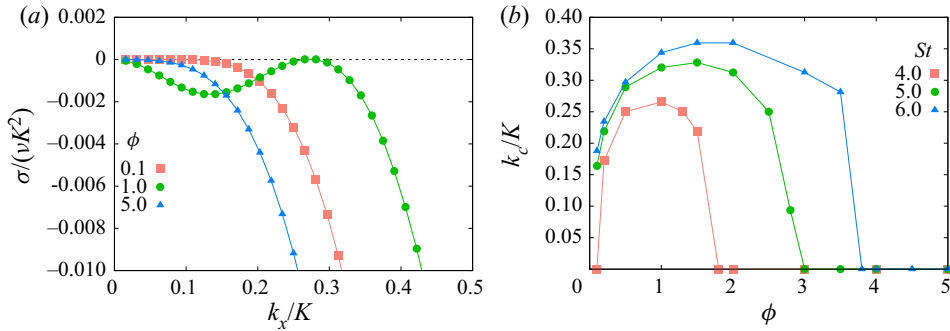
Figure 2. Panel (*a*) shows the non-dimensional growth rate $\sigma/(\nu K^2)$ as a function of the *x*-wavenumber k_x at the onset of the instability $Re = Re_c$ for $St = 4$ and different values of the mass fraction ϕ as labelled. Panel (*b*) shows the first unstable mode k_c normalized by K as a function of ϕ for different values of St as labelled.

($\phi = 0.1$ and $\phi = 5$) we observe that the growth rate σ is a monotonically decreasing function of k_x and the unstable mode is the smallest available wavenumber $k_c = k_{min} \equiv 2\pi/L$. In these cases, the hypothesis of large scale separation is justified and indeed the predictions of the multiple-scale analysis are in agreement with the numerical results. Conversely, for $\phi = 1$ the curve $\sigma(k_x)$ is non-monotonic and the unstable mode appears to be at $k_c \simeq 0.3K$, therefore the instability is no more triggered by large-scale perturbations and multiple-scale analysis fails to predict the instability. Similar behaviours have been observed also for $St = 5$ and $St = 6$ (not shown). To systematically investigate the region of parameters for which the multiple-scale analysis is not expected to work we numerically studied the dependence of the unstable (transverse) mode k_c on ϕ and St at $Re = Re_c$, shown in figure 2(*b*). For $St \geq 4$ and intermediate values of ϕ we found $k_c \simeq 0.3K$, while for $St \leq 3$ (not shown) we always found $k_c = k_{min}$ in agreement with the multiple-scale assumption. By comparing figures 2(*b*) and 1(*b*) we clearly observe the correspondence between the theoretical–numerical agreement in figure 1(*b*) and the fact that $k_c \ll K$.

6. Conclusions

We have investigated the linear stability of a dilute suspension of heavy particles in the Kolmogorov flow within the Eulerian model proposed by Saffman (1962). In the absence of particles, it is well known that the value of the critical Reynolds number $Re_c = \sqrt{2}$ for the stability of the laminar base flow can be obtained by means of a multiple-scale analysis. Here, we have adopted the same approach to extend the study of the linear stability to the full parameter space of the Saffman model given by the Reynolds number Re, the mass fraction ϕ and the Stokes number St. The multiple-scale prediction for the onset of the instability, $Re_c = \sqrt{2/((1 + \phi)^2 - \phi St)}$, as a function of St and ϕ has been compared with the results of numerical simulations of the linearized system. Figure 3 summarizes the main results. Particles with small inertia ($St < \phi + 2$, blue region) reduce the stability of the base laminar flow. Conversely, the presence of particles with large inertia ($St > \phi + 2$, red region) retards the onset of the instability. The prediction of the neutral curve $St = \phi + 2$ in which the effect of the particles on the linear stability vanishes is confirmed by numerics. In general, we have found that the multiple-scale analysis correctly predicts the values of Re_c in a large part of the parameter space. It correctly recovers the limit of a Newtonian flow with rescaled viscosity $\nu/(1 + \phi)$ both for $St \ll 1$ and $\phi \gg 1$. Nonetheless, for large St it overestimates Re_c in an intermediate range of ϕ.
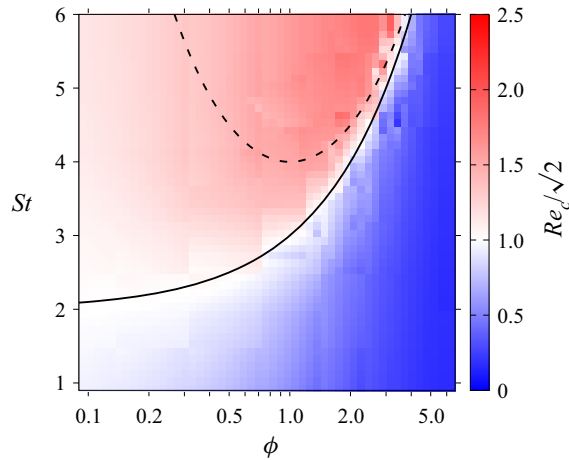
Figure 3. Critical Reynolds number as a function of ϕ and St. Red (blue) colour scale denotes regions more stable (unstable) than the Newtonian flow in which $Re_c > \sqrt{2}$ ($Re_c < \sqrt{2}$). Solid black line is the neutral curve $St = \phi + 2$ at which $Re_c = \sqrt{2}$. Dashed line represents the border of the region of unconditioned stability predicted by the multiple-scale analysis $St > (1 + \phi)^2/\phi$.

In particular, the region of unconditioned stability $St > (1 + \phi)^2/\phi$ is not observed in the numerics. By investigating numerically the dispersion relation at the critical Reynolds number, we have found that the failure of the multiple-scale prediction is due to the lack of scale separation between the most unstable mode and the wavenumber of the base flow, thus invalidating the assumptions of the perturbative approach in that parameter region. A natural extension of the present work would be to investigate the weakly nonlinear dynamics of the Kolmogorov–Saffman system and the structure of the secondary flow above Re_c (Sivashinsky 1985).

We conclude with two comments concerning the choice of the Kolmogorov base flow and the Saffman model. The first is related to the preferential concentration of inertial particles, which, in principle, can be observed also in laminar flow. For a parallel flow (such as Kolmogorov one), the fixed point solution of the model has a uniform particle density field and the infinitesimal perturbation of the density is passively transported in the linearized dynamics. Therefore, preferential concentration does not influence the linear stability of the Saffman model. To investigate such effects requires the choice of a different base flow.

The second concerns the relevance of our results to real-world systems. Modelling the coupling between the particles and the fluid in particle-laden flows is a challenging task which requires a compromise between accuracy and simplicity. The simplicity of the Saffman model combined with that of the Kolmogorov flow allowed us to obtain an analytic prediction for the critical Reynolds number. Our results could, in principle, differ quantitatively from those of more refined models (e.g. Lagrangian models with accurate implementation of the two-way coupling). Nonetheless, our work offers a qualitative benchmark for future experimental studies and numerical simulations based on Lagrangian approaches which allow us to include additional effects, such as finite particle size or particle–particle interactions, which are not captured by the Saffman model. The comparison between our results and those obtained by means of more accurate models could improve our understanding concerning the impact of such complex processes on the stability of laminar flows.

Author ORCIDs.
Ⓓ Alessandro Sozza https://orcid.org/0000-0002-6276-0641;
Ⓓ Massimo Cencini https://orcid.org/0000-0001-7073-5000.

Appendix A. Squire's theorem for the Saffman model

We consider a generic parallel basic flow $U = (U(z), 0, 0)$ in a three-dimensional domain. The linearized Saffman model around the basic flow (3.1)–(3.2) written in non-dimensional form is

$$\partial_t u + (U \cdot \nabla)u + (u \cdot \nabla)U = -\nabla p + \frac{1}{Re}\nabla u + \frac{\phi}{ReSt}(v - u), \tag{A1}$$

$$\partial_t v + (U \cdot \nabla)v + (v \cdot \nabla)U = -\frac{1}{ReSt}(v - u), \tag{A2}$$

where $Re = U/(\nu K)$ and $St = \tau \nu K^2$ and $1/K$ is the characteristic scale of $U(z)$. We now perform a Fourier transform in the directions x, y and t and write $\{u, v, p\} = \{\hat{u}(z), \hat{v}(z), \hat{p}(z)\} \exp(i k_h \cdot x_h - i\omega t)$, where $x_h = (x, y)^\mathrm{T}$ and $k_h = (k_x, k_y)^\mathrm{T}$, with T denoting the transpose. Introducing the notation $U_h = (U(z), 0)^\mathrm{T}$, $\hat{u}_h = (\hat{u}_x, \hat{u}_y)^\mathrm{T}$, and $\hat{v}_h = (\hat{v}_x, \hat{v}_y)^\mathrm{T}$, the linearized equations in normal modes take the form

$$(-i\omega + i k_h \cdot U_h)\hat{u}_h + \hat{u}_z \frac{dU_h}{dz} = -i k_h \hat{p} + \frac{1}{Re}\left(\frac{d^2}{z^2} - k_h^2\right)\hat{u}_h + \frac{\phi}{ReSt}\left(\hat{v}_h - \hat{u}_h\right), \tag{A3}$$

$$(-i\omega + i k_h \cdot U_h)\hat{u}_z = -\frac{d\hat{p}}{dz} + \frac{1}{Re}\left(\frac{d^2}{dz^2} - k_h^2\right)\hat{u}_z + \frac{\phi}{ReSt}\left(\hat{v}_z - \hat{u}_z\right), \tag{A4}$$

$$(-i\omega + i k_h \cdot U_h)\hat{v}_h + \hat{v}_z \frac{dU_h}{dz} = -\frac{1}{ReSt}\left(\hat{v}_h - \hat{u}_h\right), \tag{A5}$$

$$(-i\omega + i k_h \cdot U_h)\hat{v}_z = -\frac{1}{ReSt}\left(\hat{v}_z - \hat{u}_z\right). \tag{A6}$$

The linearized dynamics described by the (A3)–(A6) is independent for each mode k_h. Therefore, for each mode k_h it is possible to perform a rotation of the Fourier amplitudes of the velocity fields $\hat{u}_h$ and $\hat{v}_h$ in the direction of the wave vector k_h by means of the following transformation:

$$\left.\begin{array}{l} \bar{k}_x = |k_h|, \quad \bar{\omega} = \dfrac{\bar{k}_x}{k_x}\omega, \quad \overline{Re} = \dfrac{k_x}{\bar{k}_x}Re \leq Re, \\[12pt] \bar{u}_x = \dfrac{k_h \cdot \hat{u}_h}{|k_h|}, \quad \bar{u}_z = \hat{u}_z, \quad \bar{p} = \dfrac{\bar{k}_x}{k_x}\hat{p}, \quad \bar{v}_x = \dfrac{k_h \cdot \hat{v}_h}{|k_h|}, \quad \bar{v}_z = \hat{v}_z, \end{array}\right\} \tag{A7}$$

931 A26-11

From (A3)–(A6) one obtains the equations for the new variables

$$\left[-\mathrm{i}\bar{\omega} + \mathrm{i}\bar{k}_x U\right]\bar{u}_x + \bar{u}_z \frac{\mathrm{d}U}{\mathrm{d}z} = -\mathrm{i}\bar{k}_x \bar{p} + \frac{1}{Re}\left(\frac{\mathrm{d}^2}{\mathrm{d}z^2} - \bar{k}_x^2\right)\bar{u}_x + \frac{\phi}{ReSt}\left(\bar{v}_x - \bar{u}_x\right), \quad (A8)$$

$$\left[-\mathrm{i}\bar{\omega} + \mathrm{i}\bar{k}_x U\right]\bar{u}_z = -\frac{\mathrm{d}\bar{p}}{\mathrm{d}z} + \frac{1}{Re}\left(\frac{\mathrm{d}^2}{\mathrm{d}z^2} - \bar{k}_x^2\right)\bar{u}_z + \frac{\phi}{ReSt}\left(\bar{v}_z - \bar{u}_z\right), \quad (A9)$$

$$\left[-\mathrm{i}\bar{\omega} + \mathrm{i}\bar{k}_x U\right]\bar{v}_x + \bar{v}_z \frac{\mathrm{d}U}{\mathrm{d}z} = -\frac{1}{\overline{ReSt}}\left(\bar{v}_x - \bar{u}_x\right), \quad (A10)$$

$$\left[-\mathrm{i}\bar{\omega} + \mathrm{i}\bar{k}_x U\right]\bar{v}_z = -\frac{1}{\overline{ReSt}}\left(\bar{v}_z - \bar{u}_z\right). \quad (A11)$$

The new system of (A8)–(A10) is formally identical to the original one (A3)–(A6) in which one imposes a purely two-dimensional perturbation with $\hat{u}_y = \hat{v}_y = 0$ and $k_y = 0$. Therefore, three-dimensional perturbations, which are unstable at a given Re, correspond to a two-dimensional disturbance at smaller Reynolds number $\overline{Re}$ (and at the same ϕ and St) with larger growth rate ($\mathrm{Im}(\bar{\omega}) \geq \mathrm{Im}(\omega) > 0$).

REFERENCES

AGRAWAL, N., CHOUEIRI, G.H. & HOF, B. 2019 Transition to turbulence in particle laden flows. *Phys. Rev. Lett.* **122** (11), 114502.

ARDEKANI, M.N., COSTA, P., BREUGEM, W.-P., PICANO, F. & BRANDT, L. 2017 Drag reduction in turbulent channel flow laden with finite-size oblate spheroids. *J. Fluid Mech.* **816**, 43–70.

ARMITAGE, P.J. 2011 Dynamics of protoplanetary disks. *Annu. Rev. Astron. Astrophys.* **49**, 195.

BALACHANDAR, S. & EATON, J.K. 2010 Turbulent dispersed multiphase flow. *Annu. Rev. Fluid Mech.* **42**, 111–133.

BALMFORTH, N.J. & YOUNG, Y.N. 2002 Stratified Kolmogorov flow. *J. Fluid Mech.* **450**, 131.

BEC, J., LAENEN, F. & MUSACCHIO, S. 2017 Dusty turbulence. arXiv:1702.06773.

BENSOUSSAN, A., LIONS, J.-L. & PAPANICOLAOU, G. 2011 *Asymptotic Analysis for Periodic Structures*, vol. 374. American Mathematical Society.

BERCOVICI, D. & MICHAUT, C. 2010 Two-phase dynamics of volcanic eruptions: compaction, compression and the conditions for choking. *Geophys. J. Intl* **182** (2), 843–864.

BISTAGNINO, A., BOFFETTA, G., CELANI, A., MAZZINO, A., PULIAFITO, A. & VERGASSOLA, M. 2007 Nonlinear dynamics of the viscoelastic Kolmogorov flow. *J. Fluid Mech.* **590**, 61.

BOFFETTA, G., CELANI, A. & MAZZINO, A. 2005 Drag reduction in the turbulent Kolmogorov flow. *Phys. Rev.* E **71** (3), 036307.

BURNS, P. & MEIBURG, E. 2015 Sediment-laden fresh water above salt water: nonlinear simulations. *J. Fluid Mech.* **762**, 156–195.

CAPECELATRO, J., DESJARDINS, O. & FOX, R.O. 2018 On the transition between turbulence regimes in particle-laden channel flows. *J. Fluid Mech.* **845**, 499–519.

DE LILLO, F., CENCINI, M., MUSACCHIO, S. & BOFFETTA, G. 2016 Clustering and turbophoresis in a shear flow without walls. *Phys. Fluids* **28** (3), 035104.

DUBRULLE, B. & FRISCH, U. 1991 Eddy viscosity of parity-invariant flow. *Phys. Rev.* A **43**, 5355–5364.

ELGHOBASHI, S. 1994 On predicting particle-laden turbulent flows. *Appl. Sci. Res.* **52** (4), 309–329.

FYLLADITAKIS, E.D. 2018 Kolmogorov flow: seven decades of history. *J. Appl. Maths Phys.* **6** (11), 2227.

GUALTIERI, P., BATTISTA, F. & CASCIOLA, C.M. 2017 Turbulence modulation in heavy-loaded suspensions of tiny particles. *Phys. Rev. Fluids* **2** (3), 034304.

HORWITZ, J.A.K. & MANI, A. 2016 Accurate calculation of Stokes drag for point-particle tracking in two-way coupled flows. *J. Comput. Phys.* **318**, 85–109.

HUGHES, D.W. & TOBIAS, S.M. 2001 On the instability of magnetohydrodynamic shear flows. *Proc. R. Soc. Lond.* A **457**, 1365.

KLINKENBERG, J., DE LANGE, H.C. & BRANDT, L. 2011 Modal and non-modal stability of particle-laden channel flow. *Phys. Fluids* **23**, 064110.

LEGRAS, B., VILLONE, B. & FRISCH, U. 1999 Dispersive stabilization of the inverse cascade for the Kolmogorov flow. *Phys. Rev. Lett.* **82**, 4440.

LI, D., LUO, K., WANG, Z., XIAO, W. & FAN, J. 2019 Drag enhancement and turbulence attenuation by small solid particles in an unstably stratified turbulent boundary layer. *Phys. Fluids* **31** (6), 063303.

MATAS, J.P., MORRIS, J.F. & GUAZZELLI, E. 2003 Transition to turbulence in particulate pipe flow. *Phys. Rev. Lett.* **90** (1), 014501.

MESHALKIN, L.D. & SINAI, I.G. 1961 Investigation of the stability of a stationary solution of a system of equations for the plane movement of an incompressible viscous liquid. *Z. Angew. Math. Mech.* **25** (6), 1700–1705.

MICHAEL, D.H. 1964 The stability of plane Poiseuille flow of a dusty gas. *J. Fluid Mech.* **18** (1), 19–32.

MUSACCHIO, S. & BOFFETTA, G. 2014 Turbulent channel without boundaries: the periodic Kolmogorov flow. *Phys. Rev.* E **89** (2), 023004.

PANDEY, V., PERLEKAR, P. & MITRA, D. 2019 Clustering and energy spectra in two-dimensional dusty gas turbulence. *Phys. Rev.* E **100**, 013114.

RUDYAK, V.Y., ISAKOV, E.B. & BORD, E.G. 1997 Hydrodynamic stability of the Poiseuille flow of dispersed fluid. *J. Aerosol Sci.* **28** (1), 53–66.

SAFFMAN, P.G. 1962 On the stability of laminar flow of a dusty gas. *J. Fluid Mech.* **13** (1), 120–128.

SHAW, R.A. 2003 Particle-turbulence interactions in atmospheric clouds. *Annu. Rev. Fluid Mech.* **35** (1), 183–227.

SIVASHINSKY, G.I. 1985 Weak turbulence in periodic flows. *Physica* D **17** (2), 243–255.

SIVASHINSKY, G. & YAKHOT, V. 1985 Negative viscosity effect in large-scale flows. *Phys. Fluids* **28** (4), 1040–1042.

SOZZA, A., CENCINI, M., MUSACCHIO, S. & BOFFETTA, G. 2020 Drag enhancement in a dusty Kolmogorov flow. *Phys. Rev. Fluids* **5**, 094302.

SPROULL, W.T. 1961 Viscosity of dusty gases. *Nature* **190** (4780), 976–978.

SQUIRE, H.B. 1933 On the stability for three-dimensional disturbances of viscous fluid flow between parallel walls. *Proc. Math. Phys. Engng Sci.* **142**, 847.

SURI, B., TITHOF, J., MITCHELL, R. JR, Grigoriev, R.O. & Schatz, M.F. 2014 Velocity profile in a two-layer Kolmogorov-like flow. *Phys. Fluids* **26** (5), 053601.

WILKINSON, M. & MEHLIG, B. 2005 Caustics in turbulent aerosols. *Europhys. Lett.* **71** (2), 186.